Numerical study of porosity in titanium dental castings

M. WU, P. R. SAHM
Foundry Institute, University of Technology Aachen, Intzestr. 5, D-52072 Aachen, Germany
M. AUGTHUN, H. SPIEKERMANN
Department of Dental Prosthetics, University of Technology Aachen, Pauwelsstr. 30, D-52057 Aachen, Germany
J. SCHÄDLICH-STUBENRAUCH
SPACECAST Präzisionsguss GmbH, Kaiserstr. 100, D-52134, Herzogenrath, Germany

A commercial software package, MAGMASOFT (MAGMA Giessereitechnologie GmbH, Aachen, Germany), was used to study shrinkage and gas porosity in titanium dental castings. A geometrical model for two simplified tooth crowns connected by a connector bar was created. Both mold filling and solidification of this casting model were numerically simulated. Shrinkage porosity was quantitatively predicted by means of a built-in feeding criterion. The risk of gas pore formation was investigated using the numerical filling and solidification results.

The results of the numerical simulations were compared with experiments, which were carried out on a centrifugal casting machine with an investment block mold. The block mold was made of SiO_2 based slurry with a 1 mm thick ZrO_2 face coat to reduce metal–mold reactions. Both melting and casting were carried out under protective argon (40 kPa). The finished castings were sectioned and the shrinkage porosity determined. The experimentally determined shrinkage porosity coincided with the predicted numerical simulation results. No apparent gas porosity was found in these model castings.

Several running and gating systems for the above model casting were numerically simulated. An optimized running and gating system design was then experimentally cast, which resulted in porosity-free castings.

1. Introduction

The use of cast titanium (Ti) as dental prostheses has attracted an increasing and widespread interest, but porosity is still of great concern in recent laboratory research [1–4]. There are two main types of porosity in Ti castings; shrinkage porosity and gas porosity [2, 3, 5, 6].

Volumetric shrinkage upon solidification is the main cause of the porosity. If casting parameters are not properly controlled, about 1% (0.5–1.5% depending on the individual alloy's composition [5]) volumetric shrinkage creates shrinkage porosity, which tends to be distributed in the last areas to solidify.

Gas pores can be separated into two main categories: gas entrapped during mold filling and gas which is generated by metallurgical reactions. Entrapped gas, such as the inert argon cover gas, which is commonly used in Ti casting processes, follows the melt from melting chamber into the mold cavity. Entrapped gas may give rise to internal gas pores or incomplete filling of the mold cavity [7]. The gases within the mold cavity can escape either through the porous wall of the mold [6], pass out through the running and gating system as the mold cavity fills or pass out through the liquid Ti melt before a solidified skin is formed [4, 8]. Gas generated by metallurgical reactions, e.g. skin holes or subsurface porosity [9], pin holes and ''gas shrinkage'' [5], etc., appear more dispersely distributed in Ti castings, but they are often observed under the microscope.

This study focused on porosity observed at the macro scale, such as concentrated shrinkage porosity and entrapped gas porosity, which are believed to be the most harmful to dental castings.

Numerical simulation techniques provide an effective way to study the solidification sequence of dental castings [10–12]. Recent developments in coupled fluid and heat flow allow the whole casting process, from mold filling to the end of solidification to be investigated and even provide the means of predicting some casting defects [13, 14]. The aim of the study was to demonstrate that numerical simulation can be applied to dental

Corresponding author: Menghuai Wu, Gießerei-Institut, RWTH Aachen, Intzestr. 5, D-52072 Aachen, Germany.
E-mail: menghuai@gi.rwth-aachen.de.

castings and thereby allow the visualization of the filling and solidification process and the minimization of porosity levels by optimized running and gating systems.

2. Materials and methods

2.1. Numerical simulation method

2.1.1. Software

The commercial software package MAGMASOFT was used, which is supplied by MAGMA Giessereitechnologie GmbH, Aachen, Germany, which has been widely used for the simulation of industrial castings [13]. The theoretical basis of MAGMASOFT is the Navier–Stokes (fluid flow) and Fourier (heat transfer) equations, which are solved numerically by means of the finite difference method (FDM) [15, 16].

2.1.2. FDM model

A simplified geometrical model of two tooth crowns connected by a connector bar was created (Fig. 1a,b). In order to carry out the FDM simulation, the casting geometry including the casting and running and gating system were subdivided into brick like control volumes with the mesh generator in MAGMASOFT. Fig. 1(c) shows the enmeshment of 43 000 metal control volumes. A more accurate calculation needs a finer enmeshment.

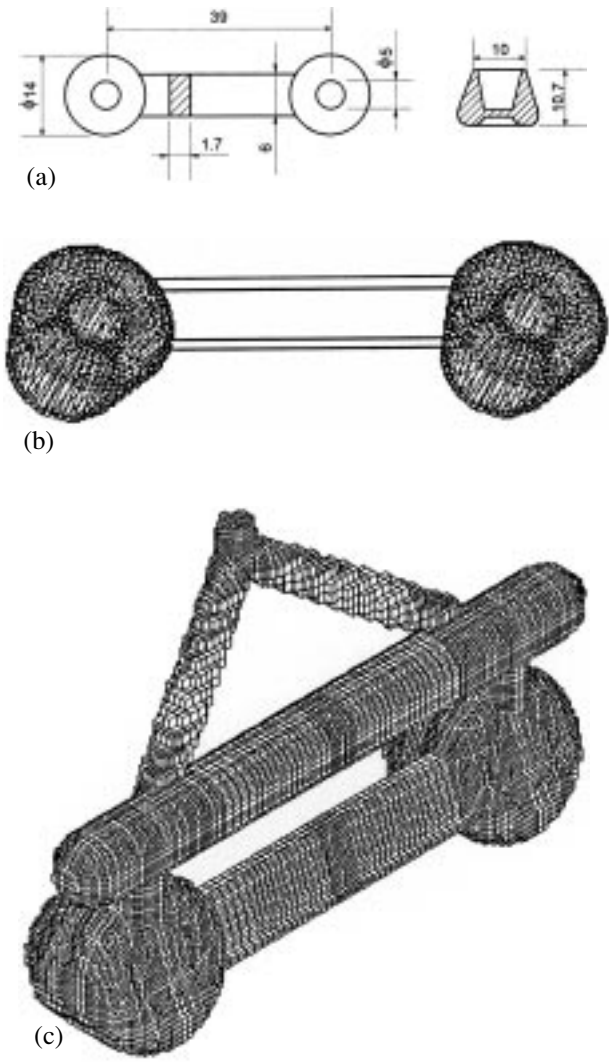

Figure 1 Geometrical model of the model casting, two simplified tooth crowns connected by a connector bar. (a) Geometrical parameters; (b) 3D wireframe model on a computer; (c) FDM mesh.

2.1.3. Porosity simulation

Shrinkage porosity was quantitatively predictable by MAGMASOFT's built-in ''feeding criterion'' function. During the simulation of the solidification of the casting, the criterion function automatically calculates the degree of solidification shrinkage and feeding for each of the control volumes. If all control volumes of the castings are 100% fed, no shrinkage will occur. If a control volume is only 95% fed for example, 5% shrinkage porosity will be seen in the control volume. There is no quantitative criterion available for gas porosity, but numerical filling and solidification results can be used to investigate the likelihood of gas entrapment and therefore the gas pore tendency.

2.1.4. Running and gating system designs

In order to optimize the design of the running and gating system for the model casting, several designs were evaluated, based on laboratory experience and literature sources [11] (Fig. 2). Design 1 was based on dental laboratory experience; Design 2 had a large sprue attached directly to each of the tooth crowns; Design 3 was similar to Design 1, but with only one shorter ingate and Design 4 was a modification of Design 3 with an increased ingate and runner bar diameter of runner 4 mm and 6 mm, respectively.

2.2. Physical and boundary conditions

2.2.1. Thermal physical data of the Ti and block mold

Commercially pure Ti ($>$ 99.4 wt %Ti, $\sim$ 0.02 wt %C, $\sim$ 0.3 wt %O, $\sim$ 0.002 wt %N, $\sim$ 0.002 wt %H, $\sim$ 0.07 wt %Fe) was used for the casting experiments. The solidification range was taken as 1660–1667 °C [17]. The latent heat of fusion was taken as 391 kJ kg^{-1}. The temperature dependent density was taken as 4506 kg m^{-3} at 20 °C, 4319 kg m^{-3} at 900 °C and 4110 kg m^{-3} above the liquidus [5]. Temperature dependent thermal conductivity was taken from literature reference [18]; and specific heat capacity from literature reference [19].

The block mold was made of SiO_2 based slurry (Giulini Chemie, Ludwigshafen, Germany) with ZrO_2 face coats of up to 1 mm thickness (Dynazirkon C, Dynamit Nobel, Troisdorf, Germany). Only a thin layer of ZrO_2 face coat was used in order to prevent the Ti from reacting with the SiO_2 based block mold (Giulini). Although the thermal conductivity of the ZrO_2 face coat is slightly higher than SiO_2, the enhancement of the total thermal conductivity by such a thin coating is considered negligible. Therefore only the thermal physical data of the SiO_2 mold was taken into account for the numerical simulation. The density of the SiO_2 mold was taken as constant at 2545 kg m^{-3}; the temperature dependent thermal conductivity and specific heat capacity were

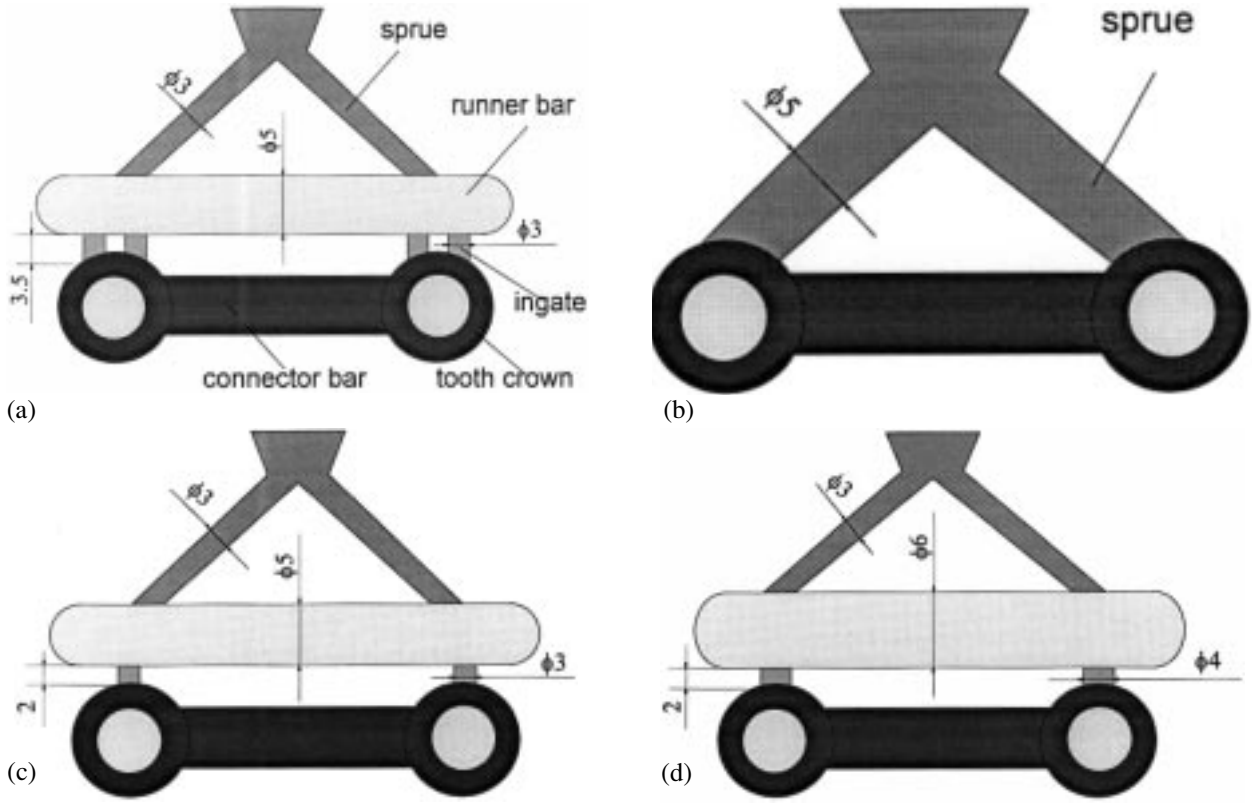

Figure 2 Different running and gating system designs for the model casting. (a) Design 1; (b) Design 2; (c) Design 3; (d) Design 4.

chosen from the MAGMASOFT database (MAGMA Giessereitechnologie GmbH, Aachen, Germany).

2.2.2. Initial temperature and velocity at the inlet

The initial conditions for simulation were taken as the mold preheat temperature of 500 °C and the Ti pouring temperature of 1700 °C [12].

For the boundary condition for mold filling, the velocity v at the inlet of the casting must be calculated. Fig. 3 shows schematically the filling process of the centrifugal casting machine. The centrifugal radius R, was 115 mm, the maximum rotation speed w was 360 r.p.m., the crucible seat angle $\theta < 10°$ and the acceleration distance l (from the exit of the crucible to the inlet) was 26 mm. In order to allow the melt to flow over the crucible and fill the mold cavity, the centrifugal force F_c has to be large enough for the free surface of the liquid metal to be at least parallel to the side wall of the crucible, i.e.

$$\tan\theta = \frac{g}{a_R} \tag{1}$$

where g is acceleration due to gravity 9.81 m s^{-2}, a_R is centrifugal acceleration; and θ is crucible seat angle.

Taking into account the centrifugal acceleration a_R of the melt and the acceleration distance l, the velocity v at the inlet can be estimated as

$$v = (2la_R)^{1/2} = \left(\frac{2gl}{\tan\theta}\right)^{1/2} \tag{2}$$

In practice, the crucible seat angle θ is maintained below 10°, i.e. the filling velocity will be greater than 1.7 m s^{-1}.

2.3. Casting experiments

The wax patterns (Lunacast, Fuller GmbH, Lüneburg, Germany) were firstly coated with face coat slurry consisting of ZrO_2 flour (Dynazirkon C, Dynamit Nobel, Troisdorf, Germany) and binder (Titanbond, SPACECAST Präzisionsguss GmbH, Herzogenrath, Germany). After drying the face coat layer under natural convection for 3 h, the patterns were placed in a muffle (casting ring), and the SiO_2 based slurry (Giulini Chemie, Ludwigshafen, Germany) was poured into the muffle under vacuum (10 kPa) with mild vibration. Dewaxing and high temperature sintering of the block mold were all carried out in a furnace (Combilabor, Heraeus, Hanau, Germany) according to the manufacturer's recommended program, then the block mold was held at the preheat temperature (recommended 500 °C [12]) before being transferred to the casting machine. For

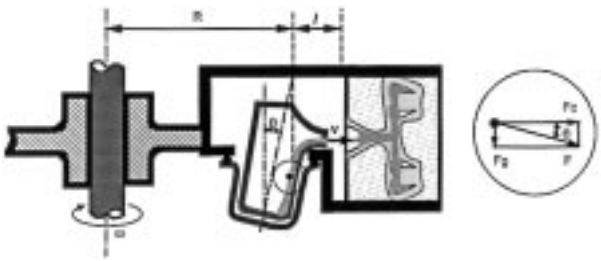

Figure 3 A schematic diagram of the centrifugal filling process.

each running and gating system design five castings were made with the same set of casting parameters.

The castings were made on a centrifugal casting machine (Titancast, Linn High-Therm, Eschenfelden, Germany). The casting procedure is briefly described below.

1. Load 23 g of pure Ti billet into the graphite crucible;
2. Mount the preheated mold in the casting machine;
3. Evacuate the melting chamber to a vacuum of 1 Pa;
4. Fill the chamber with Ar up to a pressure of 40 kPa;
5. Start the high frequency induction melt with a color pyrometer to monitor the temperature (accuracy of $\pm$ 10 °C);
6. Start the centrifugal casting machine and fill the mold cavity.

After casting, the mold was air-cooled. The mold was carefully knocked out and the remaining mold material was removed by sand blasting.

The finished castings were cut and polished through the tooth crown in several layers of about 2 mm thickness to detect the concentrated shrinkage porosity under microscope. Micrographs were taken to show the distribution of the shrinkage porosity.

3. Results

3.1. Mold filling calculations and porosity prediction

Filling sequence of the casting and the Design 4 running and gating system (Fig. 2d) are shown in Fig. 4. After 0.05 s, 30% of the mold cavity is filled, at which point the ingates connecting the runner bar and tooth crowns were only partially filled. In this case the gas in the crowns can easily escape away through the unfilled part of the ingates into the runner bar. After 0.1 s, at which point the mold cavity was 60% filled, the ingates were completely filled. The gas entrapped must either pass through the permeable block mold, or move through the liquid Ti to the top most surface before a solidification skin blocks its escaping path. The last areas to fill are indicated by arrows in Fig. 4(c). Due to the high filling rate of the centrifugal casting machine, the whole mold cavity was completely filled within 0.145 s. The coupled heat and fluid flow simulations show the temperature loss as quite high during such a short filling period, especially at the tip of the tooth crown, but the melt remains above the melting point and no solidification occurs during the filling process.

Solidification isotherms of the Design 1 are shown when 70% of the casting is solidified in Fig. 5. White areas $(T > T_L)$ show areas still in the liquid state; black areas $(T < T_s)$ show areas of 100% solidified Ti; and areas between T_L and T_s are ''mushy''. The feeding path from the runner bar, which also acts as a reservoir for feed metal, to the tooth crown was blocked during the later stages of solidification at the narrowest section in the ingates. Shrinkage porosity was predicted by MAGMASOFT's built-in feeding criterion (Fig. 6a). By slicing through the casting model in small steps, it was found that most of the casting was well fed, but the

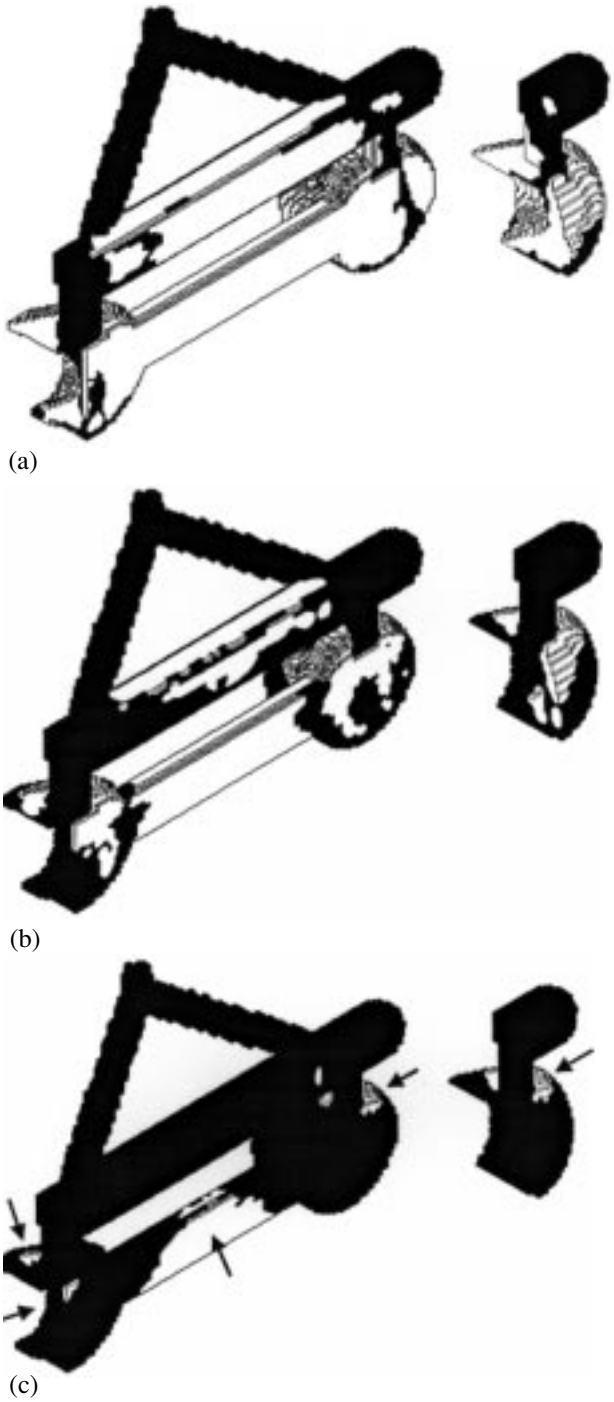

Figure 4 Numerical simulation results of the mold filling. Arrows indicate the last areas to fill. (a) 30% filled (0.05 s); (b) 60% filled (0.1 s); (c) 90% filled (0.14 s).

Figure 5 The temperature distribution in the tooth crown when the whole casting was 70% solidified: Design 1.

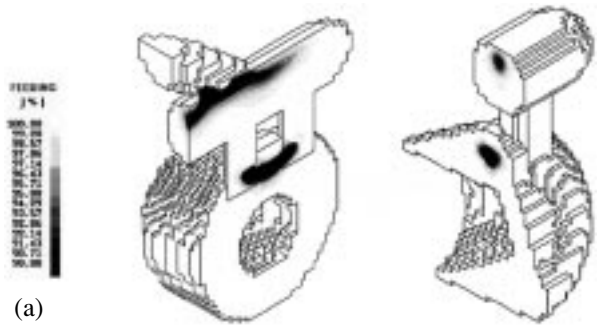

(a)

(b)

Figure 6 A comparison between computer predicted and experimentally determined porosity levels: Design 1. (a) Shrinkage porosity prediction; (b) Experiment determined shrinkage porosity.

(a)

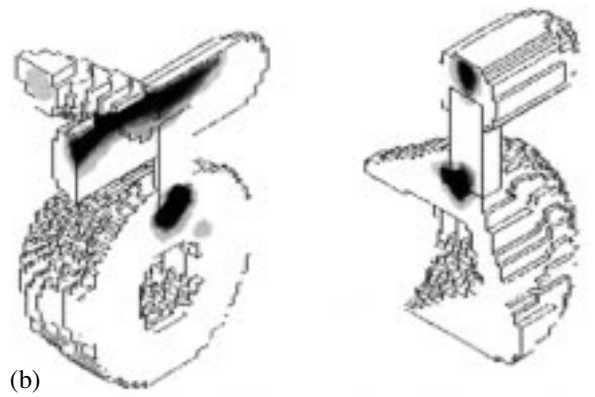

(b)

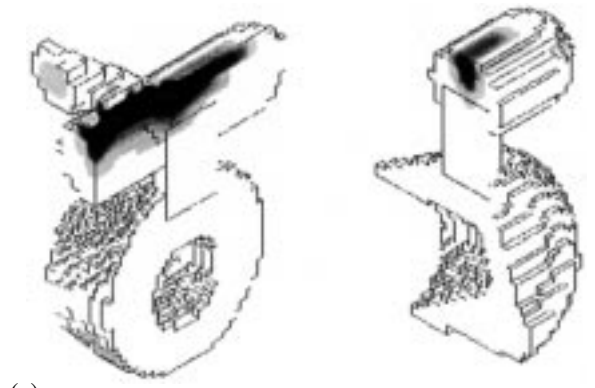

(c)

Figure 7 Computer-aided running and gating system optimization. A comparison of the computer predicted shrinkage porosity levels in the tooth crown for different running and gating system designs. (a) Predicted shrinkage in Design 2; (b) Predicted shrinkage in Design 3; (c) No apparent shrinkage was predicted in Design 4.

area between the two ingates was only 91 to 96% fed, i.e. 4–9% of the volumetric shrinkage porosity. Casting experiments were conducted and the results are shown by the micrograph, Fig. 6(b), in which similar shrinkage levels can be seen. No gas pores were found in the crowns.

3.2. Simulation results of different running and gating system designs

Simulations were carried out on the different designs, and a summary of the results is shown in Fig. 7. In Design 2, no additional feeding measures were taken with only one large sprue being attached to each crown. Even though the diameter of the sprue was 5 mm, porosity was still indicated by the simulation at the sprue-crown junction (Fig. 7a). Theoretically it would be possible to move the hot spot from this junction into the sprue by increasing the size of the sprue, but this was not practical, and therefore it was not carried out in the trial casting. In Design 3, there was still some shrinkage porosity in the vicinity of the ingate-crown junction (Fig. 7b). Design 4 was the best design, with no shrinkage porosity predicted in the casting by the simulation (Fig. 7c). In total 5 castings with this design were experimentally cast, and no shrinkage or gas porosity was found in the castings. The computer predicted results compared well with the casting experiments.

4. Discussion

4.1. Mold filling, solidification and porosity prediction

Porosity is formed during the mold filling and solidification of dental castings. It is difficult, even impossible to observe the mold filling and solidification in such a thin-walled dental casting experimentally, but numerical simulation provides an effective means of doing this.

As shown in the results of the mold filling simulation (Fig. 4), the last areas to fill are easily identified. Gas tends to be entrapped in these regions and forms gas bubbles in the liquid melt. If these bubbles can not pass out of the casting and penetrate through the mold before solidification blocks the escape path, gas pores will be

present in the casting. Shrinkage porosity is quantitatively predictable. The computer predicted shrinkage porosity level coincided well with the experimental determined levels. Therefore it has been demonstrated that the numerical model of the software and the applied thermal physical data for the simulations are reliable. Previous experimental research [1–4] revealed that both shrinkage and gas pores are responsible for porosity in Ti dental castings. However, our experiments seem to indicate that only shrinkage porosity is of concern for this model casting, as no gas pores were found in the crown model. The main reasons are discussed below.

1. The high reactivity and affinity of Ti for the elements O, N and H and reactions between Ti and the block mold would contribute to gas pores in Ti castings [6]. The use of an inert mold, such as the ZrO_2 coating used in this study and a suitable burnout and preheating procedure [12] may have reduced the metallurgical reactions during mold filling and solidification.

2. The centrifugal force imposed on the melt enhances the removal of gas bubbles which may be generated during the filling of the mold cavity [20, 21]. Reportedly the number of gaseous defects can be reduced to a negligible level with a centrifugal force of $30\,\boldsymbol{g}$ ($\boldsymbol{g} = 9.81\,\mathrm{m\,s^{-2}}$) [20]. In this case, when the machine reached its maximum rotation speed, the centrifugal acceleration a_R in the mold cavity was

$$a_R = \frac{\pi^2 w^2 R}{900} \tag{3}$$

The maximum rotation speed w of Titancast is 360 r.p.m., a typical centrifugal radius R of a dental casting on this machine is 0.19–0.23 m, therefore, the maximum centrifugal acceleration is estimated to be $270–326\,\mathrm{m\,s^{-2}}$, i.e. $28–34\,\boldsymbol{g}$. This may cause the gas bubbles to be compressed into microscopically small pores, which are then not seen.

3. The wall thickness used in this model (Fig. 1a) was thicker than an occlusal surface of a real crown, because the thicker wall thickness of the occlusal surface tends to get more porosity. The whole filling process (Fig. 4) took 0.145 s. No premature solidification occurred in this short period. It took about 5 s for the crown to solidify completely, during which there seems to be enough time for the entrapped gas to escape out of the casting.

4.2. Running and gating system design

The design of the running and gating system used was considered as an empirical method, which was not well understood [12]. There are many possible designs available for different dental castings [11], but the commonly used designs were found to be inadequate for Ti casting [3]. In this study two simplified crowns connected by a connector bar were simulated in order to investigate the capability and validate the numerical simulation method for sprue optimization (Fig. 2).

As a first design each dental crown was filled through two separate ingates of $\phi 3$ mm, which were connected to a runner bar of $\phi 5$ mm (Fig. 2a). The runner bar was intentionally designed to prevent the initial high velocity metal stream from rushing directly into mold cavity, thereby reducing the turbulence, which may induce gas bubbles or slag inclusions formation in the mold cavity. Moreover it served as a source of feed metal to the casting. The two ingates for each crown were designed to enhance the feeding efficiency. However, both simulation and experiments indicated that porosity occurred near and beneath the ingates in the crowns. Obviously the geometrical parameters of Design 1 were not optimal for this model casting (Fig. 6).

Another alternative is Design 2, which is shown in Fig. 2b. The simulation results indicated that this Design is not desirable. In order to move the porosity from the ingate-crown junction into the sprue, a relatively large sprue is necessary. This is not desirable from the point of view of dental practice, as the contour of the crown has to be reformed manually at the junction between the sprue and the crown. The post casting processing of an even larger area of the crown would be even more time consuming and expensive.

For the model casting only Design 4 (Fig. 2d) is recommended. An ideal solidification sequence from casting to ingate and finally towards the horizontal runner bar occurs. No porosity was predicted in the crown by the simulations (Fig. 7c), and porosity free castings were obtained experimentally.

Both the numerical simulation and casting experiments reveal that the running and gating system design plays a very important role in porosity control in Ti dental castings. With the help of the numerical simulation used in this work it was possible to visualize the mold filling process and solidification sequence on the screen, to investigate the influence of the running and gating system design and to optimize the design for porosity free Ti dental castings.

Acknowledgments

The authors would like to express their gratitude to the German Government for the sponsorship of this work within the BIOMAT project No. 15. The authors would also like to thank MAGMA Giessereitechnologie GmbH for their technical support and service. Special thanks are given to Ms B. Gaspart for her work in performing the experiments.

References

1. H. HERØ, M. SYVERUD and M. WAARLI, *J. Mater. Sci.: Mater. Med.* **4** (1993) 296.
2. *Idem.*, *Dent. Mater.* **9** (1993) 15.
3. T. I. CHAI and R. S. STEIN, *J. Prosth. Dentistry* **73** (1995) 534.
4. I. WATANABE, J. H. WATKINS, H. NAKAJIMA, M. ATSUTA and T. OKABE, *J. Dent. Res.* **76** (1997) 773.
5. O. N. MAGNITSKIY, in ''Casting properties of titanium alloys'', edited translation (CLEARING-HOUSE for Federal Scientific and Technical Information Springfield, VA, 1970) pp. 5 and 92.
6. M. SYVERUD and H. HERØ, *Dent. Mater.* **11** (1995) 14.
7. K. WATANABE, S. OKAWA, O. MIYAKAWA, S. NAKANO, N. SHIOKAWA and M. KOBAYASHI, *Dent. Mater. J.* **10** (1991) 128.
8. J. CAMPBELL, in ''Castings'' (Butterworth Heinemann, London, 1991) 16.
9. O. MIYAKAWA, K. WATANABE, S. OKAWA, S. NAKANO, H. HONMA, M. KOBAYASHI and N. SHIOKAWA, *Dent. Mater. J.* **12** (1993) 171.
10. M. AUGTHUN, L. BECKER, H. KREUTZER, P. R. SAHM, W.

SCHÄFER and J. SCHÄDLICH-STUBENRAUCH, *Deutsche Zahnärztliche Zeitschrift* **44** (1989) 849.
11. H. KREUTZER, W. SCHÄFER, J. SCHÄDLICH-STUBENRAUCH and P. R. SAHM, *Dent. Lab.* **37** (1989) 908.
12. J. SCHÄDLICH-STUBENRAUCH and P. R. SAHM, *Giessereiforschung* **43** (1991) 141.
13. P. R. SAHM, in ''Formfüll- und Erstarrungs-simulation–Ein Übersicht, Guss-Produkte'94'' (Hoppenstedt *Co., Darmstadt-Berlin, 1994) 237.
14. P. N. HANSEN, G. C. HARTMANN and J. C. STURM, *AFS Trans*. **99** (1991) 477.
15. D. M. LIPINSKI, W. SCHÄFER and E. FLENDER, in Proceedings of 4th International Conference on Modeling of Casting, Welding and Advanced Solidification Process, Florida, USA, March 21–26, 1993, p.389.
16. P. R. SAHM and P. N. HANSEN, in ''Numerical simulation and modeling of casting and solidification process for foundry and cast-house'' (Comite Int. des Associations Techniques de Fouderie, Zurich, 1984).
17. R. BOYER, G. WELSCH and E. W. COLLINGS, in ''Materials properties handbook: titanium Alloys'' (ASM International, Materials Park, 1994) 125.
18. Y. S. TOULOUKIAN, R. W. POWELL, C. Y. HO and P. G. KLEMENS, in ''Thermophysical properties of matter: thermal conductivity-metallic elements and alloys'', The TPRC Data Series (1) p.414.
19. Y. S. TOULOUKIAN and E. H. BUYCO, in ''Thermophysical properties of matter: specific heat-metallic elements and alloys'', The TPRC Data Series (4) p.260.
20. K. SUZUKI, K. NISHIKAWA and S. WATAKABE, *Mater. Trans. JIM* **37** (1996) 1793.
21. J. TAKAHASHI, J. Z. ZHANG and M. OKAZAKI, *Dent. Mater. J.* **12** (1993) 245.
22. J. D. PRESTON and R. BERGER, *Dent. Clin. North Am.* **21** (1977) 717.

Received 25 May
and accepted 20 July 1998